A dynamical approach to the exterior geometry of a perfect fluid as a relativistic star

Mohsen Fathi[1)]

Department of Physics, Islamic Azad University, Central Tehran Branch, Tehran, Iran

Abstract: In this article, we assume that a cold charged perfect fluid is constructing a spherical relativistic star. Our purpose is the investigation of the dynamical properties of its exterior geometry, through simulating the geodesic motion of a charged test-particle, while moving on the star.

Key words: astrophysics, relativistic stars, geodesics

PACS: 04.20.-q **DOI:** 10.1088/1674-1137/37/2/025101

1 Introduction

The einstein field equation leads to the solutions satisfying the definition of a perfect fluid; a homogenous isotropic mass and energy distribution with no viscosity, such as Friedmann-Lemaître model (for a good review see Ref. [1]). Moreover, it also provides the chance to investigate the interior distributions of the perfect fluid through the energy-momentum tensor, not forgetting that the energy-momentum tensor can actually be extracted from charged bodies bearing interior pressure.

A relativistic star is supposed to consist of such a fluid either charged or with axial rotation [2]. In order to find out the relativistic, isotropic mass and charge the interior solution has been suggested by B. Guilfoyl [3].

In this article, we are about to form a static charged relativistic star using these so-called solutions; in addition, studying the dynamical properties of the exterior geometry via a rotating test-particle is included.

It goes without saying that in general relativity geodesic motions are of great importance. This is because they make valuable predictions about cases such as precessions of periastron in planetary orbits and theoretical explanations for light deflection in gravitational fields.

Furthermore, there is a lot of researches which has been dedicated to the study of geodesic motions in different kinds of geometrical background, which could be derived from general relativity, for example, Schwarzchild, Schwarzchild-de Sitter, Reissner-Nordström and Kerr geometries (see Refs. [4]–[8] and an important text book [9]). The exact equations of motion have also been derived [10], and lots of further theoretical predictions provided (see Refs. [11]–[17]).

In this case we are considering Reissner-Nordström (RN) geometry as the exterior geometry of a static charged relativistic star. The procedure that we are going through in this paper concerns the process in which charged particles get trapped in gravitational and electrical fields of relativistic stars.

The chosen approach is a Lagrangian formalism and numerical simulations also have been involved. In order to do so, three classes of solutions presented by Guilfoyl have been utilized to construct a relativistic star and to compare the pertinent geodesic behaviors of the test charged particle.

The article is organized as follows: Section 2 contains dynamical preliminaries for a charged particle in RN geometry. Section 3 considers a brief review on Guilfoyl's interior solutions. In Section 4, we introduce the Lagrangian formalism. Finally, Sections 5 and 6, consist of the simulations of the charged particle's motions on various types of relativistic stars.

2 Charged particle in RN geometry

First, let us consider a spherical source which has been schematically illustrated in Fig. 1. It indicates the charged star, considered to be the gravitational source, with R_0 being the radius, and the total mass and charge being m_0 and q_0 respectively. A test-particle which is moving on this star, is assumed to travel on the RN geodesics. The RN geometry is a static spherically symmetric vacuum solution for the Einstein equations in four dimensions (d=4) and is defined by the metric:

$$\mathrm{d}s^2=-c^2A(r)\mathrm{d}t^2+B(r)\mathrm{d}r^2+r^2\mathrm{d}\theta^2+r^2\sin^2\theta\mathrm{d}\phi^2, \quad (1)$$

in which the variable coefficients are:

Received 27 March 2012, Revised 30 May 2012

1) E-mail: mohsen.fathi@gmail.com

$$A(r)=\frac{1}{B(r)}=1-\frac{2Gm_0}{rc^2}+\frac{q_0^2G}{4\pi\epsilon_0 r^2c^4},$$

where G stands for the gravitational constant and c for the speed of light. In order to simplify the calculations, we use geometrical units, fixing:

$$G=c=\frac{1}{4\pi\epsilon_0}=1.$$

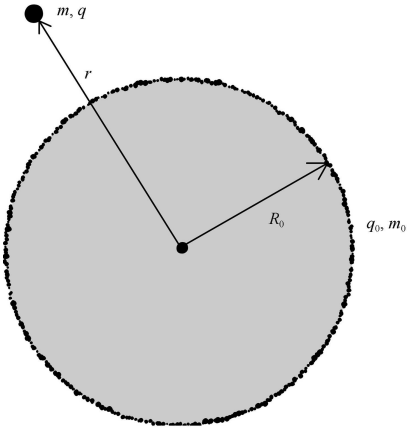

Fig. 1. A schematic illustration of a charged spherical star and rotating test charged particle.

According to these units, one can relate length dimensions to quantities like mass and electric charge, i.e. (see Ref. [18] Appendix 4):

$$[\text{mass}]=[m_0]=\ell,$$

$$[\text{electric charge}]=[q_0]=\ell,$$

where ℓ notates the length dimension. Since c and G are supposed to be 1, the remaining ratios $\frac{2m_0}{r}$ and $\frac{q_0^2}{r^2}$, become dimensionless. These assumptions are commonly used in general relativity. Taking these into account, one can rewrite (1) as:

$$\mathrm{d}s^2 = -\left(1-\frac{2m_0}{r}+\frac{q_0^2}{r^2}\right)\mathrm{d}t^2+\left(1-\frac{2m_0}{r}+\frac{q_0^2}{r^2}\right)^{-1}\mathrm{d}r^2 +r^2\mathrm{d}\Omega^2. \quad (2)$$

We will use this metric in further considerations.

If we write the Killing equations for Killing vector X_μ, as [19]:

$$(\nabla_\mu X)_\nu+(\nabla_\nu X)_\mu=0, \quad (3)$$

one can obtain 10 Killing vectors for the spacetime defined by metric (2). Therefore, since for the RN spacetime we have $d=4$, the number of Killing vectors would be $\frac{d(d+1)}{2}$. Due to this fact, the RN spacetime has Killing symmetry and we can define energy and obtain time-like geodesics.

By considering the characteristics of the test-particle (m stands for the mass and q for the charge), one can obtain the potential and energy conditions, using the Hamilton-Jacobi equation of wave crests [20]:

$$g^{\mu\nu}(P_\mu+qA_\mu)(P_\nu+qA_\nu)+m^2=0. \quad (4)$$

P_μ is the momentum 4-vector[1)]

$$P_\mu=g_{\mu\sigma}P^\sigma=g_{\mu\sigma}\frac{\mathrm{d}x^\sigma}{\mathrm{d}\lambda}. \quad (5)$$

Here λ is the affine parameter of the trajectory. The metric components $g_{\mu\nu}$ can be derived from the exterior geometry of the source, the RN metric (2). Also the vector potential A_μ for the static charged source will be:

$$A_\mu=(\varphi(r),0,0,0), \quad (6)$$

where $\varphi(r)=\frac{q_0}{r}$ is the scalar electrical potential, outside the star, producing a scalar field within the spacetime. One can define the two conserved quantities as:

$$E=-P_0, \quad (7)$$

the energy, and

$$L=P_\phi \quad (L\geqslant 0), \quad (8)$$

the angular momentum. Here we consider $\theta=\frac{\pi}{2}$, for which the particle's motion is confined to the equatorial rotations. Therefore

$$P^\theta=\frac{\mathrm{d}\theta}{\mathrm{d}\lambda}=0.$$

Substituting the metric (2) in (4) yields:

$$-\frac{\left(E-\frac{qq_0}{r}\right)^2}{1-\frac{2m_0}{r}+\frac{q_0^2}{r^2}}+\left(1-\frac{2m_0}{r}+\frac{q_0^2}{r^2}\right)^{-1}\left(\frac{\mathrm{d}r}{\mathrm{d}\lambda}\right)^2 +\frac{L^2}{r^2}+m^2=0,$$

or

$$\left(\frac{\mathrm{d}r}{\mathrm{d}\lambda}\right)^2=\left(E-\frac{qq_0}{r}\right)^2-\left(1-\frac{2m_0}{r}+\frac{q_0^2}{r^2}\right)\left(m^2+\frac{L^2}{r^2}\right). \quad (9)$$

Eq. (9) can be rewritten as:

$$\left(\frac{\mathrm{d}r}{\mathrm{d}\lambda}\right)^2 = \left[E-\left(\frac{qq_0}{r}-\sqrt{\left(1-\frac{2m_0}{r}+\frac{q_0^2}{r^2}\right)\left(m^2+\frac{L^2}{r^2}\right)}\right)\right] \times\left[E-\left(\frac{qq_0}{r}+\sqrt{\left(1-\frac{2m_0}{r}+\frac{q_0^2}{r^2}\right)\left(m^2+\frac{L^2}{r^2}\right)}\right)\right].$$

1) Here we use the notation in Ref. [20], in which in §25.3 the 4-momentum has been defined like Eq. (5).

We introduce the potential, felt by the test-particle as:

$$V(r)=\frac{qq_0}{r}+\sqrt{\left(1-\frac{2m_0}{r}+\frac{q_0^2}{r^2}\right)\left(m^2+\frac{L^2}{r^2}\right)}, \tag{10}$$

to be assured that positive potential is available. To discuss the motion of the test-particle also, we need the rate of variation of rotation angle ϕ with respect to r. Previously we defined:

$$g_{\phi\phi}P^{\phi}=L\Rightarrow\frac{\mathrm{d}\phi}{\mathrm{d}\lambda}=\frac{L}{r^2}.$$

Substituting in Eq. (9) yields:

$$\left(\frac{\mathrm{d}r}{\mathrm{d}\phi}\right)^2=\frac{r^4}{L^2}\left[\left(E-\frac{qq_0}{r}\right)^2-\left(1-\frac{2m_0}{r}+\frac{q_0^2}{r^2}\right)\left(m^2+\frac{L^2}{r^2}\right)\right]. \tag{11}$$

Solutions to equations like (11), have been obtained using the Weierstrass function and elliptic integrals in [10], however in this context, we use a Lagrangian formalism instead of the geodesic equations.

For different values of L and E, the test-particle experiences different types of motions. The motion of the particle, depends on its energy, for sets of solutions for $E-V(r)=0$. The RN spacetime allows three types of orbits; for one zero, we will have scape orbits, for two zeros, periodic bound orbits are available, and for three zeros, we will have scape/capture orbits and periodic bound orbits.

The potential that the particle is going through is also worthy of investigation. The potential may have some extremum points, as below:

$$\left.\frac{\mathrm{d}V(r)}{\mathrm{d}r}\right|_{(r=r_{\mathrm{e}})}=0. \tag{12}$$

We can rewrite the potential in Eq. (10) as:

$$V(r)=C(r)+\sqrt{g(r)\left(m^2+\frac{L^2}{r^2}\right)}. \tag{13}$$

We have $C(r)=\dfrac{qq_0}{r}$ and $g(r)=1-\dfrac{2m_0}{r}+\dfrac{q_0^2}{r^2}$. Using (13) in (12) forms the following differential equation:

$$C'\sqrt{g\left(m^2+\frac{L^2}{r^2}\right)}+\frac{1}{2}\left[g'\left(m^2+\frac{L^2}{r^2}\right)-2\frac{gL^2}{r^3}\right]=0.$$

Solving the above equation for L yields:

$$L=r\left(\frac{2r^2gC'^2-r^2g'^2m^2+2g'm^2gr\pm2\sqrt{r^4g^2C'^4-2r^3g^2C'^2g'm^2+4g^3r^2m^2C'^2}}{r^2g'^2-4g'rg+4g^2}\right)^{\frac{1}{2}}. \tag{14}$$

This solution, corresponds to the stable orbits of the test-particle around the star, where the potential has its extremum points. The expression for L in Eq. (14) indicates that, for stable orbits regardless of the energy of the particle, the total angular momentum, for definite values of mass, charge and radius of the source, can take only definite values. As we will see, the energy of the particle is peculiar, when we work with a particular potential.

We are going to discuss the types of motions in Section 5, considering different interior mass and charge distributions for the star. We shall introduce these interior solutions in the next section.

3 Weyl-type interior solutions for a charged perfect fluid

In this article, a relativistic star, is defined to be a charged spherically symmetric cold perfect fluid. Such a fluid is a solution of the Einstein field equations

$$R_{\mu\nu}-\frac{1}{2}g_{\mu\nu}R=8\pi(T_{\mu\nu}+E_{\mu\nu}), \tag{15}$$

and the Maxwell equations

$$\nabla_\nu F^{\mu\nu}=4\pi J^\mu, \tag{16}$$

for a charged isotropic mass distribution. In Eq. (15), $E_{\mu\nu}$ is the electromagnetic stress-energy tensor, defined as [20]:

$$4\pi E_{\mu\nu}=F_\mu^\rho F_{\nu\rho}-\frac{1}{4}g_{\mu\nu}F_{\rho\sigma}F^{\rho\sigma}, \tag{17}$$

in which

$$F_{\mu\nu}=\nabla_\mu A_\nu-\nabla_\nu A_\mu,$$

is the antisymmetric electromagnetic field strength tensor. The energy-momentum tensor for an isotropic mass distribution with pressure is:

$$T_{\mu\nu}=\begin{pmatrix}\rho&0&0&0\\0&p&0&0\\0&0&p&0\\0&0&0&p\end{pmatrix}, \tag{18}$$

where ρ is the matter density and p is the fluid pressure. The following spherically symmetric metric is assumed to explain the interior geometry of the perfect fluid:

$$\mathrm{d}s^2=-\omega^2\mathrm{d}t^2+\xi(r)^2\mathrm{d}r^2+r^2\mathrm{d}\Omega^2, \tag{19}$$

in which the metric potential

$$\omega(\varphi)^2=a+b\varphi+\varphi^2, \tag{20}$$

by Weyl's assumption [22], only depends on the electric potential $\varphi(r)$, and a and b in (20) are constants.

The non-zero components of Maxwell Eq. (16) for metric (19), determine the total charge inside a volume

with radius r. We have [23]:

$$Q(r)=\frac{r^2\varphi'(r)}{\omega(\varphi)\xi(r)}=4\pi\int_0^r\sigma(r)r^2\xi(r)\mathrm{d}r, \tag{21}$$

in which $\sigma(r)$ is the volume charge density. Since outside the star, the geometry obeys the RN metric (2), Eq. (21) can be rewritten as

$$Q(r)=r^2\varphi'(r)[A(r)B(r)]^{-\frac{1}{2}}.$$

According to the Weyl's assumption in (20), this gives:

$$\varphi'(r)=\mp\frac{A'(r)}{\sqrt{b^2+4A(r)-4a}}.$$

Therefore

$$Q(r)=\mp A'(r)\{A(r)B(r)(b^2+4A(r)-4a)\}^{-\frac{1}{2}}. \tag{22}$$

Now to realize what the interior solutions of a relativistic star really are, let us consider another star, with radius r_0 ($r_0=R_0+\delta r$), charge Q_0 and mass M which are considered to be known values. This star (Fig. 2) is not the one that will be used as the massive source for the test-particle to move on. It is only used for discussing the interior solutions and it is in fact, a boundary condition to derive the desired constants in the interior solutions. However, the massive source in Fig. 1 has the same distributions but in lower dimensions. The radius r_0 will be considered to be the same for all cases, therefore the stars under discussion will have the same geometrical appearance and obviously the amounts Q_0 and M will differ for different interior solutions. Now for the star in Fig. 2, the continuity condition at $r=r_0$ implies that:

$$A(r_0)=\frac{1}{B(r_0)}=1-\frac{2M}{r_0}+\frac{Q_0^2}{r_0^2},$$

in which $Q_0=Q(r_0)$. Therefore, from Eq. (22) we obtain:

$$\frac{M}{Q_0}=\pm\frac{1}{2}\sqrt{b^2+4(1-aQ_0^2)}, \tag{23}$$

which implies that for $a=b=0$ we have:

$$M=|Q_0|.$$

This is the condition concerning a Majumdar-Papapetrou star for a Weyl-type metric potential. The pressure for these stars is zero; in this case the relation between the metric potential ω^2 in (20) and the electrical potential $\varphi(r)$ is always a perfect square [24, 25]. Also we will discuss the motion of the test-particle around these stars in Section 5.

In Ref. [3], Guilfoyl has presented some interesting Weyl-type interior solutions for a spherically symmetric charged perfect fluid. He based his solutions on two presuppositions:

1) The Schwarzchild condition which implies:

$$8\pi T_{00}-8\pi E_{00}=\frac{3}{R^2}=\text{constant},$$

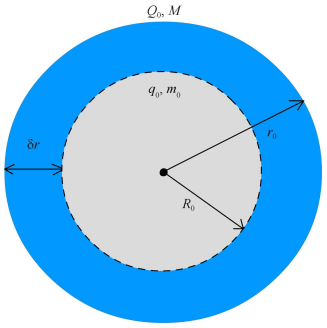

Fig. 2. A star with higher dimensions, having the same distributions as Fig. 1, but with known values for charge and mass.

or

$$8\pi\rho(r)+\frac{Q(r)^2}{r^4}=\frac{3}{R^2}=\text{constant}. \tag{24}$$

2) The expression for the radial part of metric (19):

$$\xi(r)^2=\left(1-\frac{r^2}{R^2}\right)^{-1}. \tag{25}$$

In these two presuppositions, the quantity $\frac{1}{R^2}$, is a constant that must be determined using the boundary conditions at $r=r_0$ (in Fig. 2). We now bring up two classes of Guilfoyl's solutions which we will use later to form the test-particle's potential [3]:

3.1 The case of Class I

In this case, the metric potential is considered to have the spherical form:

$$a\omega^2=b+(c+\varphi)^2, \tag{26}$$

where c is a constant. We call this the Weyl-Guilfoyl metric potential as it is in Ref. [23]. Both using the RN limit in (19) and also considering (26) we have:

$$\frac{M}{Q_0}=\frac{Q_0}{ar_0}(a-1)\pm\frac{1}{ar_0}\sqrt{r_0^2(a-b)+Q_0^2(1-a)}. \tag{27}$$

As we can see, while $a=1$ and $b=0$ we have $M=|Q_0|$ which is the Majumdar condition. For the expression (26), two sets of solutions have been introduced:

Class Ia: $a=\frac{1}{2}$, $b=0$

$$\begin{cases}\omega^2=\mathrm{e}^{\sqrt{2}\psi(r)}\\ Q(r)=\pm\dfrac{kr^3}{2}\\ 8\pi\rho(r)=\dfrac{3}{R^2}-\dfrac{k^2r^2}{4}\end{cases}. \tag{28}$$

The function $\psi(r)$ is defined as:

$$\psi(r)=l-kR^2\left(1-\frac{r^2}{R^2}\right)^{\frac{1}{2}}. \tag{29}$$

Also the constants $\frac{1}{R^2}$, k and l can be determined, using the boundary conditions at $r=r_0$ (Fig. 2) as below:

$$k = \frac{2|Q_0|}{r_0^3}, \tag{30}$$

$$l = \left(\frac{M}{Q_0}-\frac{Q_0}{2r_0}\right)^{-1}\left(1-\frac{2M}{r_0}+\frac{Q_0^2}{r_0^2}\right)^{\frac{1}{2}} + \sqrt{2}\ln\left(1-\frac{2M}{r_0}+\frac{Q_0^2}{r_0^2}\right), \tag{31}$$

$$\frac{1}{R^2} = \frac{2}{r_0^3}\left(M-\frac{Q_0^2}{2r_0}\right). \tag{32}$$

Class Ib: $a=1$, $b<0$

$$\begin{cases} \omega^2=-b\tan^2[\sqrt{-b}\psi(r)] \\ Q(r)=\pm\sqrt{-b}kr^3\sec[\sqrt{-b}\psi(r)] \\ 8\pi\rho(r)=\frac{3}{R^2}+bk^2r^2\sec^2[\sqrt{-b}\psi(r)] \end{cases}. \tag{33}$$

The solution set Class Ib, are confirmed for

$$b\leqslant 0 \Leftrightarrow M\geqslant |Q_0|.$$

The corresponding coefficients are:

$$b=1-\left(\frac{M}{Q_0}\right)^2, \tag{34}$$

$$k=\frac{Q_0^2}{r_0^3}\left(M-\frac{Q_0^2}{r_0}\right)^{-1}, \tag{35}$$

$$l=\left[\left(\frac{M}{Q_0}\right)^2-1\right]^{-\frac{1}{2}}\sec^{-1}\left[\left(\frac{M}{Q_0}-\frac{Q_0}{r_0}\right)\left\{\left(\frac{M}{Q_0}\right)^2-1\right\}^{-\frac{1}{2}}\right] + \left(1-\frac{2M}{r_0}+\frac{Q_0^2}{r_0^2}\right)^{\frac{1}{2}}\left(\frac{M}{Q_0}-\frac{Q_0}{r_0}\right)^{-1}\left(\frac{2M}{Q_0}-\frac{Q_0}{r_0}\right)^{-1}. \tag{36}$$

3.2 The case of Class II

In this case Guilfoyl assumed that the metric potential ω^2 has the following form:

$$\frac{\sqrt{2}}{3}a\omega^{\frac{3}{2}}=c+\varphi(r). \tag{37}$$

The interior solutions for this case are:

$$\begin{cases} \omega^2=\frac{1}{a^4}[\ln(-a^2\psi(r))]^2 \\ Q(r)=\pm\frac{kr^3}{\sqrt{2}\psi(r)}[-\ln(-a^2\psi(r))]^{-\frac{1}{2}} \\ 8\pi\rho(r)=\frac{3}{R^2}-\frac{k^2r^2}{2\psi(r)^2}[-\ln(-a^2\psi(r))]^{-1} \end{cases}. \tag{38}$$

Also the constant coefficients are:

$$a = \sqrt{2}\left(\frac{M}{Q_0}-\frac{Q_0}{r_0}\right)^{-1}\left(1-\frac{2M}{r_0}+\frac{Q_0^2}{r_0^2}\right)^{\frac{1}{4}}, \tag{39}$$

$$k = \frac{1}{r_0^3}\left(M-\frac{Q_0^2}{r_0}\right)\exp\left[-2\left(\frac{M}{Q_0}-\frac{Q_0}{r_0}\right)^{-2}\left(1-\frac{2M}{r_0}+\frac{Q_0^2}{r_0^2}\right)\right], \tag{40}$$

$$l = \frac{1}{2}\left(\frac{M}{Q_0}-\frac{Q_0}{r_0}\right)\left(1-\frac{2M}{r_0}+\frac{Q_0^2}{r_0^2}\right)^{\frac{1}{2}}\left[\left(\frac{M}{Q_0}-\frac{Q_0}{2r_0}\right)^{-1} - \left(\frac{M}{Q_0}-\frac{Q_0}{r_0}\right)\left(1-\frac{2M}{r_0}+\frac{Q_0^2}{r_0^2}\right)^{-1}\right] \times\exp\left[-2\left(\frac{M}{Q_0}-\frac{Q_0}{r_0}\right)^{-2}\left(1-\frac{2M}{r_0}+\frac{Q_0^2}{r_0^2}\right)\right]. \tag{41}$$

We use these interior solutions in Section 5, to form different types of relativistic stars.

4 Lagrangian formalism for a charged particle moving in RN spacetime

Now let us consider a Lagrangian like:

$$\mathcal{L}=\frac{1}{2}mu_iu^i-V(r), \tag{42}$$

where $u^i=\frac{\mathrm{d}x^i}{\mathrm{d}\lambda}$ is the velocity 4-vector for the test-particle and $V(r)$ is the potential in (10). One can write down this equation for the RN spacetime as:

$$\mathcal{L}=\frac{1}{2}mg_{ii}(u^i)^2-V(r), \tag{43}$$

in which the diagonal components of the metric (2) are used. Therefore the Lagrangian is a function like:

$$\mathcal{L}\equiv\mathcal{L}(t,r,\theta,\phi,\dot{t},\dot{r},\dot{\theta},\dot{\phi}). \tag{44}$$

Here the dot stands for differentiation with respect to affine parameter λ in geodesic motion. Using the RN metric (2) yields:

$$\mathcal{L} = \frac{1}{2}m\left(-1+2\frac{m_0}{r}-\frac{{q_0}^2}{r^2}\right)\dot{t}^2+\frac{1}{2}m\dot{r}^2\left(1-2\frac{m_0}{r}+\frac{{q_0}^2}{r^2}\right)^{-1} +\frac{1}{2}mr^2\dot{\theta}^2+\frac{1}{2}mr^2(\sin(\theta))^2\dot{\phi}^2-\frac{qq_0}{r} -\sqrt{\left(1-2\frac{m_0}{r}+\frac{{q_0}^2}{r^2}\right)\left(m^2+\frac{L^2}{r^2}\right)}. \tag{45}$$

Since we take the geometrical units, we have $\mathrm{d}\lambda=\mathrm{d}\tau$, where τ is the proper time. The action in this spacetime, therefore, is defined by [21]:

$$S=\int\mathcal{L}(t,r,\theta,\phi,\dot{t},\dot{r},\dot{\theta},\dot{\phi})\mathrm{d}\tau, \tag{46}$$

turning to the following one for equatorial rotations:

$$S=\int\mathcal{L}(t,r,\phi,\dot{t},\dot{r},\dot{\phi})\mathrm{d}\tau. \tag{47}$$

Varying this action, we can obtain the Euler-Lagrange equation of motion in RN spacetime:

$$\frac{\partial\mathcal{L}}{\partial x^i}-\frac{\mathrm{d}}{\mathrm{d}\tau}\left(\frac{\partial\mathcal{L}}{\partial\dot{x}^i}\right)=0. \tag{48}$$

For i=0, 1, 3, this leads to three equations which together are the equations of equatorial motion $\left(\theta=\frac{\pi}{2}\right)$ for the test-particle, moving in RN geometry. Using the definition of the potential in (10), and the Lagrangian (45) in (48) we have:

$$\begin{aligned}
&\left(-2\frac{m_0\frac{\mathrm{d}}{\mathrm{d}\tau}r(\tau)}{(r(\tau))^2}+2\frac{{q_0}^2\frac{\mathrm{d}}{\mathrm{d}\tau}r(\tau)}{(r(\tau))^3}\right)\frac{\mathrm{d}}{\mathrm{d}\tau}t(\tau)+\left(-1+2\frac{m_0}{r(\tau)}-\frac{{q_0}^2}{(r(\tau))^2}\right)\frac{\mathrm{d}^2}{\mathrm{d}\tau^2}t(\tau)=0,\\
&-m\left(\frac{\mathrm{d}}{\mathrm{d}\tau}r(\tau)\right)\left(2\frac{m_0\frac{\mathrm{d}}{\mathrm{d}\tau}r(\tau)}{(r(\tau))^2}-2\frac{{q_0}^2\frac{\mathrm{d}}{\mathrm{d}\tau}r(\tau)}{(r(\tau))^3}\right)\left(1-2\frac{m_0}{r(\tau)}+\frac{{q_0}^2}{(r(\tau))^2}\right)^{-2}\\
&+m\frac{\mathrm{d}^2}{\mathrm{d}\tau^2}r(\tau)\left(1-2\frac{m_0}{r(\tau)}+\frac{{q_0}^2}{(r(\tau))^2}\right)^{-1}-\frac{1}{2}m\left(-2\frac{m_0}{(r(\tau))^2}+2\frac{{q_0}^2}{(r(\tau))^3}\right)\left(\frac{\mathrm{d}}{\mathrm{d}\tau}t(\tau)\right)^2\\
&+\frac{1}{2}m\left(\frac{\mathrm{d}}{\mathrm{d}\tau}r(\tau)\right)^2\left(2\frac{m_0}{(r(\tau))^2}-2\frac{{q_0}^2}{(r(\tau))^3}\right)\left(1-2\frac{m_0}{r(\tau)}+\frac{{q_0}^2}{(r(\tau))^2}\right)^{-2}\\
&-mr(\tau)\left(\frac{\mathrm{d}}{\mathrm{d}\tau}\phi(\tau)\right)^2-\frac{qq_0}{(r(\tau))^2}+\frac{1}{2}\left[\sqrt{\left(1-2\frac{m_0}{r(\tau)}+\frac{{q_0}^2}{(r(\tau))^2}\right)\left(m^2+\frac{L^2}{(r(\tau))^2}\right)}\right]\\
&\times\left[\left(2\frac{m_0}{(r(\tau))^2}-2\frac{{q_0}^2}{(r(\tau))^3}\right)\left(m^2+\frac{L^2}{(r(\tau))^2}\right)-2\left(1-2\frac{m_0}{r(\tau)}+\frac{{q_0}^2}{(r(\tau))^2}\right)L^2(r(\tau))^{-3}\right]=0,\\
&2r(\tau)\left(\frac{\mathrm{d}}{\mathrm{d}\tau}\phi(\tau)\right)\frac{\mathrm{d}}{\mathrm{d}\tau}r(\tau)+(r(\tau))^2\frac{\mathrm{d}^2}{\mathrm{d}\tau^2}\phi(\tau)=0.
\end{aligned} \tag{49}$$

Using various interior solutions, in the next section we solve these equations of motion numerically, for a particle moving on a relativistic star (Fig. 1), and obtain the shape of possible orbits due to different available potentials.

5 Moving charge on a relativistic star: various interior solutions

Now let us come back to our original source, i.e. the star with radius $r=R_0$ (Fig. 1). We will illustrate the orbits of a massive charged particle, moving around this star. The interior distributions in the star, obey the three cases of interior solutions discussed in Section 3. Since we have discussed the interior solutions for a star with radius r_0, for the total charge amount of the star in Fig. 1 we have:

$$q_0=Q(R_0)=Q(r_0-\delta r), \tag{50}$$

in which $Q(r)$ is one of the interior solutions introduced in Section 3. Also for this star's total mass we have [3]:

$$m_0=\frac{1}{2}\int_0^{R_0}r^2\mathrm{d}r\left(8\pi\rho(r)+\frac{Q(r)^2}{r^4}\right)+\frac{q_0^2}{2R_0}.$$

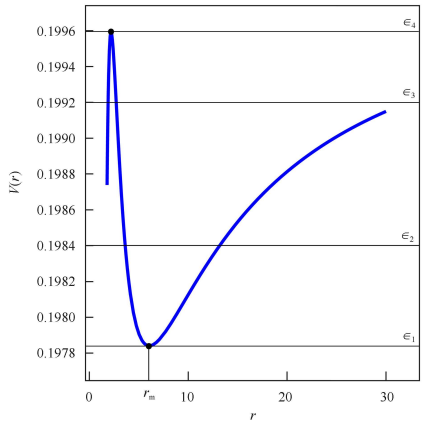

Fig. 3. The potential for a test-particle moving on a relativistic star, with the interior solution Class Ia. The illustration is plotted for Q_0=0.85, q=0.18 ,m=0.2 , L=0.225 ,r_0=2, δr=0.1r_0. The unit of length along the coordinate axis is M.

Using Eq. (24) this can be summarized as:

$$m_0=\frac{(r_0-\delta r)^3}{2R^2}+\frac{q_0^2}{2(r_0-\delta r)}, \tag{51}$$

where $\frac{1}{R^2}$ was determined in (32). In the rest of this section we will discuss different sources.

5.1 For Class Ia

In this case the total charge q_0 can be derived from the general formula (50) using Class Ia solution, namely Eqs. (28)–(32):

$$q_0=\frac{Q_0(r_0-\delta r)^3}{{r_0}^3}. \tag{52}$$

The total mass m_0 has the same relation as (51). We should notice that in our investigations we suppose that the final amounts of charge and mass, Q_0 and M, have the same ratio $\left(\frac{Q_0}{M}\right)$ in all considered cases, to facilitate the comparison of interior solutions. The potential in (10), for an intermediate angular momentum, is shown in Fig. 3. Falling in this potential, the test-particle can access three types of orbits, due to the total energy E (notated in Fig. 3).

1) Periodic bound orbits

This type of orbit, is often called planetary orbit, especially when the shape of trajectories, is elliptical. Fig. 4 shows some possible bound orbits for different values of initial energy E.

2) Hyperbolic motion

For particles coming from infinity, hyperbolic motions or escape orbits are available. That is when $E-V(r)=0$ possesses only one zero. Fig. 5 shows some possible types of escape orbits, for which the particle comes to the vicinity of the star, having a definite minimum distance, and then repels again to the infinity.

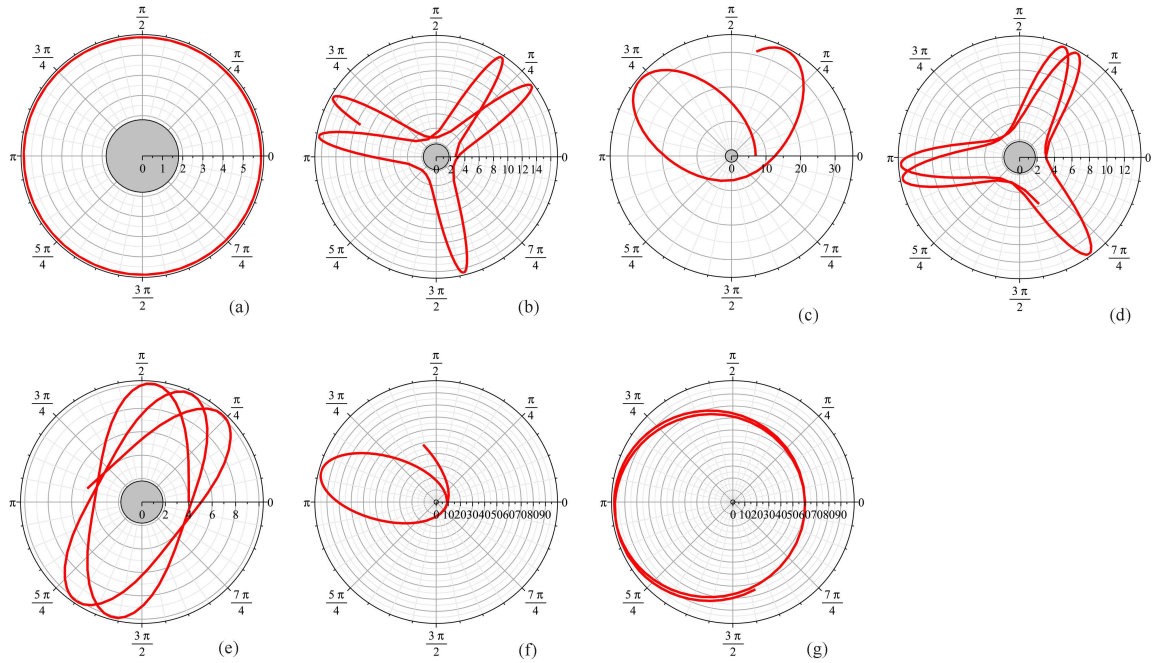

Fig. 4. The possible bound orbits (or planetary orbits) for a test-particle moving on a star with interior solution Class Ia, using different initial points of approach and different initial energies: (a) $r=r_{\rm m}$, $E=\epsilon_1$; (b) $r=2.7$, $E=\epsilon_1$; (c) $r=7$, $E=\epsilon_2$; (d) $r=3$, $E=\epsilon_3$; (e) $r=4$, $E=\epsilon_4$; (f) $r=9$, $E=0.36$; (g) $r=60$, $E=10$.

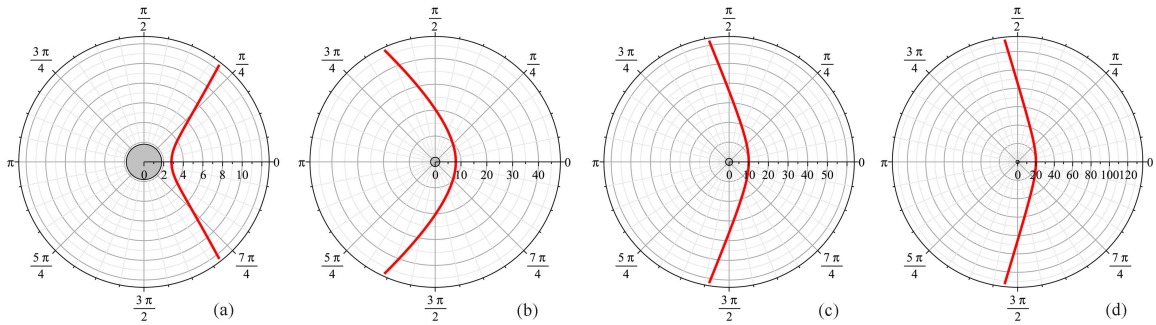

Fig. 5. The possible escape orbits (or hyperbolic motions) for a test-particle approaching a star with interior solution Class Ia, using different initial points of approach and different initial energies: (a) $r=2.8$, $E=\epsilon_3$; (b) $r=8$, $E=\epsilon_4$; (c) $r=10$,$E=\epsilon_2$; (d) $r=20$, $E=0.9$.

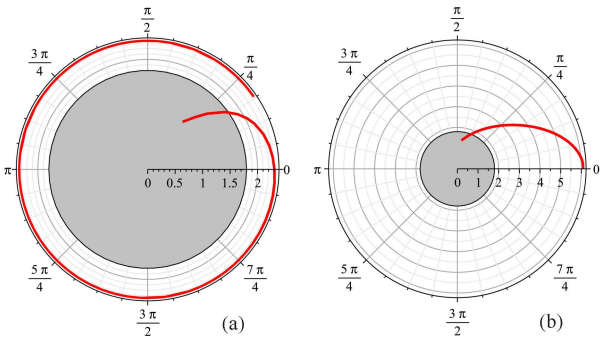

Fig. 6. The terminating orbits (or capture) for a test-particle approaching a star with interior solution Class Ia, using different initial points of approach and different initial energies: (a) r=2.197, E=ϵ_4; (b) r=$r_{\rm m}$, E=0.9.

3) Terminating orbits

Having high energies, when the particle moves in the vicinity of the star, terminating orbits are also possible. This type of orbit is unstable and terminates when the particle falls on the star's surface (being captured). Fig. 6 shows this type of motion for different energies.

5.2 For Class Ib

The total charge of the star, using Eqs. (33)–(36) is:

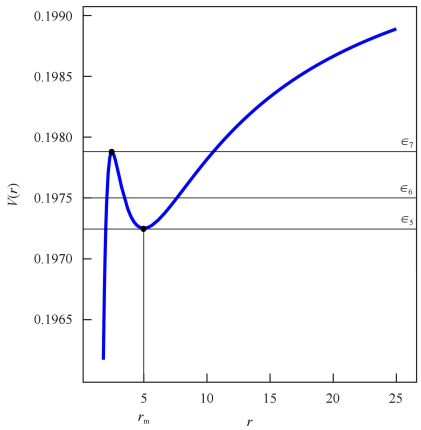

Fig. 7. The potential for a test-particle moving on a relativistic star, with the interior solution Class Ib. The illustration is plotted for Q_0=0.85, q=0.18, m=0.2, L=0.225, r_0=2, δr=0.1r_0. The unit of length along the coordinate axis is M.

$$q_0 = r_0^{-3}\left[M-\frac{Q_0^2}{r_0}\right]^{-1}\sqrt{\frac{M^2}{Q_0^2}-1}Q_0{}^2(r_0-\delta r)^3\sec\left(\sqrt{\frac{M^2}{Q_0^2}-1}\left\{\sec^{-1}\left(\left[\frac{M}{Q_0}-\frac{Q_0}{r_0}\right]\frac{1}{\sqrt{\frac{M^2}{Q_0^2}-1}}\right)\frac{1}{\sqrt{\frac{M^2}{Q_0^2}-1}}\right.\right.$$
$$+\sqrt{1-2\frac{M}{r_0}+\frac{Q_0{}^2}{r_0^2}}\left(\frac{M}{Q_0}-\frac{Q_0}{r_0}\right)^{-1}\left(2\frac{M}{Q_0}-\frac{Q_0}{r_0}\right)^{-1}$$
$$\left.\left.-Q_0\sqrt{1-(r_0-\delta r)^2Q_0\left(2\frac{M}{Q_0}-\frac{Q_0}{r_0}\right)r_0^{-3}}\left(M-\frac{Q_0{}^2}{r_0}\right)^{-1}\left(2\frac{M}{Q_0}-\frac{Q_0}{r_0}\right)^{-1}\right\}\right). \quad (53)$$

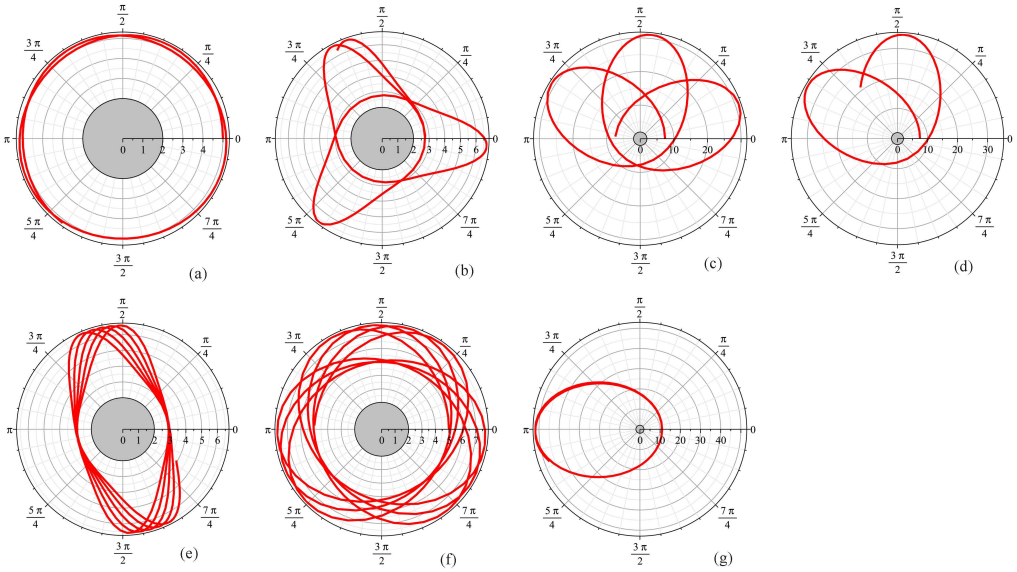

Fig. 8. The possible bound orbits (or planetary orbits) for a test-particle moving on a star with interior solution Class Ib, using different initial points of approach and different initial energies: (a) $r=r_{\rm m}$, $E=\epsilon_5$; (b) $r=2.75$, $E=\epsilon_5$; (c) r=7.4 ,$E=\epsilon_5$; (d) r=7.5, $E=\epsilon_6$; (e) r=2.9, $E=\epsilon_7$; (f) $r=r_{\rm m}$, $E=\epsilon_7$; (g) r=11, E=0.6.

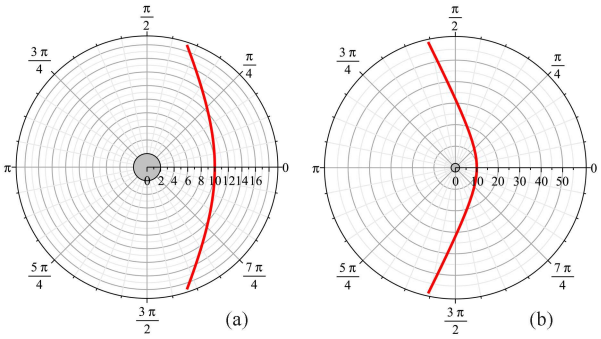

Fig. 9. The possible escape orbits (or hyperbolic motions) for a test-particle approaching a star with interior solution Class Ib, using different initial points of approach and different initial energies: (a) r=10, E=ϵ_5; (b) r=10, E=ϵ_7.

Utilizing the same data which were used to plot the potential in Fig. 3, can lead us to the potential for Class Ib, shown in Fig. 7. For a particle moving on a star with Class Ib as the interior solutions, the so-called three types of orbits are also available. The periodic bound orbits (shown in Fig. 8), the scape orbit (shown Fig. 9) and the capture (shown in Fig. 10).

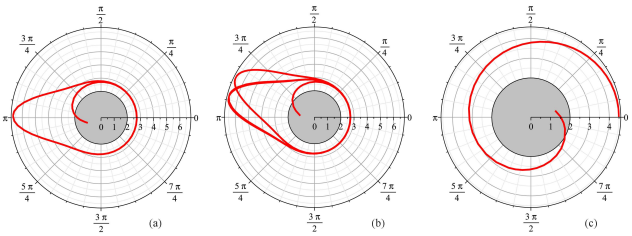

Fig. 10. The terminating orbits (or capture) for a test-particle approaching a star with interior solution Class Ib, using different initial points of approach and different initial energies: (a) r=2.725, E=ϵ_5; (b) r=2.729, E=ϵ_7; (c) r=4.5, E=0.3.

5.3 For Class II

The total charge in this case, using Eqs. (38)–(41) is:

$$\begin{aligned} q_0 \;=\; & (-r_0^2+2Mr_0-Q_0^2)(2Mr_0-Q_0^2)Q_0^2\sqrt{2}(r_0-\delta r)^3 \\ & \times\Big(2-Xr_0^2Q_0^2+XQ_0^2Mr_0-XQ_0^4+2XM^2r_0^2+2YQ_0^2r_0^2-4YQ_0^2Mr_0+2YQ_0^4\Big)^{-1} \\ & \times\Bigg[-r_0^8\ln\Bigg(-\frac{r_0^2X}{(Mr_0-Q_0^2)(2Mr_0-Q_0^2)(-r_0^2+2Mr_0-Q_0^2)}\Big\{-2Xr_0^2Q_0^2 \\ & +XQ_0^2Mr_0-XQ_0^4+2XM^2r_0^2+2YQ_0^2r_0^2-4YQ_0^2Mr_0+2YQ_0^4\Big\}\mathrm{e}^{\frac{2Q_0^2(-r_0^2+2Mr_0-Q_0^2)}{(Mr_0-Q_0^2)^2}}\Bigg)\Bigg]^{-\frac{1}{2}}, \end{aligned} \tag{54}$$

in which

$$X=\sqrt{-\frac{2Mr_0-Q_0^2-r_0^2}{r_0^2}},\; Y=\sqrt{-\frac{2r_0^3M-r_0^4-r_0^2Q_0^2-4r_0^2\delta rM+2r_0\delta rQ_0^2+2\delta r^2Mr_0-\delta r^2Q_0^2}{r_0^4}}.$$

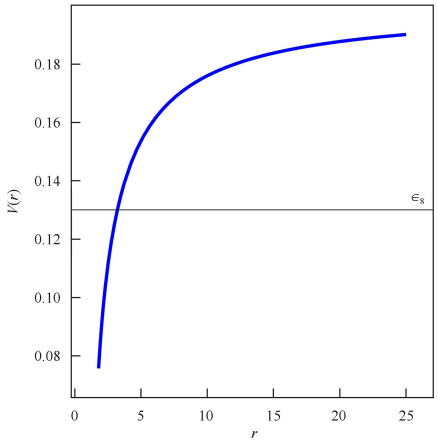

Fig. 11. The potential for a test-particle moving on a relativistic star, with the interior solution Class II. The illustration is plotted for Q_0=0.85, q=0.18, m=0.2, L=0.225, r_0=2, δr=0.1r_0. The unit of length along the coordinate axis is M.

The corresponding potential for the same data used before, has been illustrated in Fig. 11. According to this potential, the equation $E-V(r)=0$ possesses only one zero. Therefore, it is expected that the particle exhibits only unstable orbits (escape and terminating orbits). However, for medium and high energies, when the particle comes from infinity, the periodic bound orbits are also available. All types of possible orbits have been indicated in Fig. 12.

6 Motion of a charged particle on a Majumdar-Papapetrou star

Our last discussion, belongs to the stars with a special case of interior solutions Class Ia, corresponding to the Weyl-Guilfoyle spherically symmetric metric potential in Eq. (26). From Eq. (27) one can confirm that for such

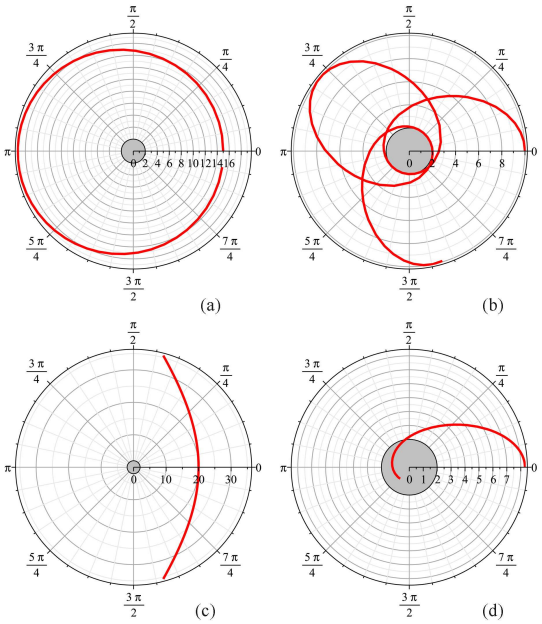

Fig. 12. The possible orbits for a test-particle moving on a star with interior solution Class II, using different initial points of approach and different initial energies: (a), (b) the periodic bound orbits for $r=15$, $E=\epsilon_8$ and $r=10$, $E=0.3$; (c) the escape orbit for $r=20$, $E=\epsilon_8$; (d) the terminating orbit for $r=8.3$, $E=\epsilon_8$.

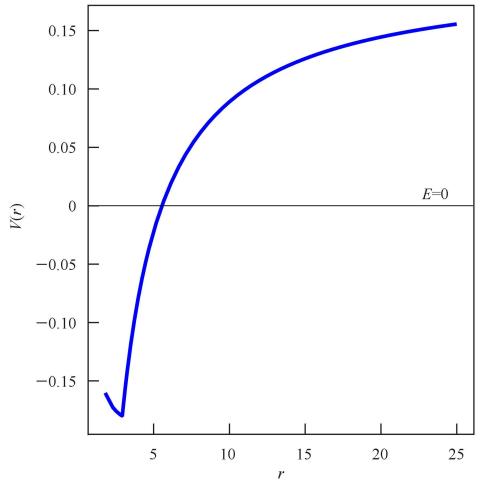

Fig. 13. The potential for a test-particle moving on a Type 1 Majumdar-Papapetrou star. The interior solution is Class Ia considering the first case $l=+kR^2$. The illustration is plotted for $Q_0=-1$, $q=0.18$, $m=0.2$, $L=0.124$, $r_0=2$, $\delta r=0.1r_0$. The unit of length along the coordinate axis is M.

metric, the conditions $a=1$ and $b=0$ form a star with equal total mass and charge, i.e.

$$M=|Q_0|.$$

This condition for a pressure-less charged perfect fluid, is the Majumdar condition [24, 25]. In this case, the relation between the metric potential $\omega(\varphi)^2$ and the electric potential $\varphi(r)$ is a perfect square:

$$\omega(\varphi)^2=(c+\varphi)^2,$$

where c is a constant. In this section we generally investigate the potential for a massive charged particle moving on a Majumdar-Papapetrou star. In order to do so, we consider the shrunk star (the inner circle in Fig. 1), to apply the interior solution. We use also the Class Ia solution with $a=1, b=0$ from Ref. [3]. The solution is:

Class Ia: $a=1$, $b=0$

$$\begin{cases} \omega^2=-[\psi(r)]^{-2} \\ Q(r)=\mp\dfrac{kr^3}{\psi(r)} \\ 8\pi\rho(r)=\dfrac{3}{R^2}-\dfrac{k^2r^2}{\psi(r)^2} \end{cases}, \tag{55}$$

in which the function $\psi(r)$ was defined in (29). Since $M=|Q_0|$, for this class of solutions, the constant coefficients are as follows:

$$k = \frac{|Q_0|}{r_0^3}\left(1-\frac{|Q_0|}{r_0}\right)^{-1}, \tag{56}$$

$$l^2 = k^2R^4, \tag{57}$$

in which

$$\frac{1}{R^2}=\frac{2|Q_0|}{r_0^3}\left(1-\frac{|Q_0|}{2r_0}\right). \tag{58}$$

As before we use the default solution of $Q(r)$. Here the default solution is the negative one. There would be two cases:

I) The case $l=+kR^2$ (Type 1):

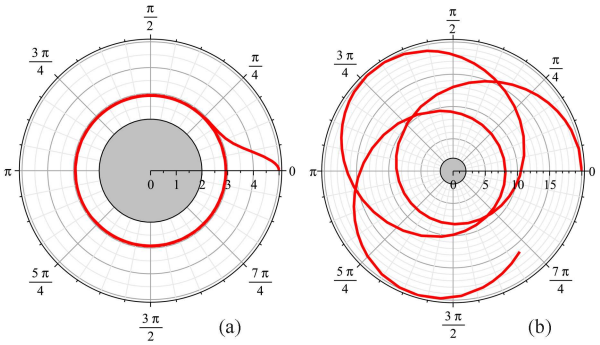

Fig. 14. Periodic bound orbits for a test-particle moving on a type 1 Majumdar-Papapetrou star, using different initial points of approach when $E=0$: (a) circular orbits for $r=5$, $E=0$; (b) $r=20$, $E=0$.

In this case the total charge of the star is:

$$q_0=Q(r_0-\delta r)=-\frac{k(r_0-\delta r)^3}{\left(l-kR^2\sqrt{1-\dfrac{(r_0-\delta r)^2}{R^2}}\right)}. \tag{59}$$

Using Eqs. (55)–(57) we obtain:

$$q_0=-\frac{(-2r_0+|Q_0|)(r_0-\delta r)^3|Q_0|}{r_0^4}\left[\sqrt{\frac{r_0^4-2|Q_0|r_0^3+r_0^2Q_0^2+4|Q_0|r_0^2\delta r-2r_0\delta rQ_0^2-2|Q_0|\delta r^2r_0+\delta r^2Q_0^2}{r_0^4}}-1\right]^{-1}. \quad (60)$$

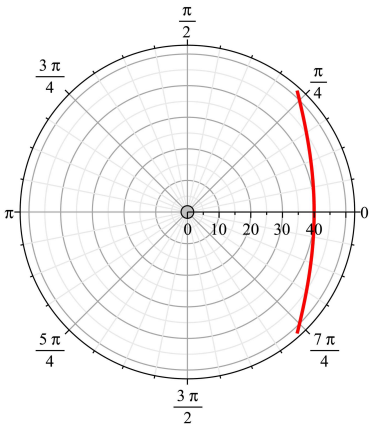

Fig. 15. The escape orbits for a test-particle moving on a Type 1 Majumdar-Papapetrou star for: $r=40$, $E=0$.

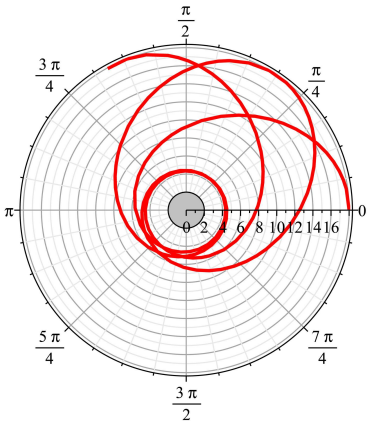

Fig. 16. The periodic bound orbits for higher energies for a test-particle moving on a Type 1 Majumdar-Papapetrou star taking: $r=18$, $E=0.2$.

The total mass can also be calculated using Eq. (51). This leads us to conclude:

$$m_0=|q_0|,$$

which is predictable. The corresponding potential is illustrated in Fig. 13. The minus part of the potential is of no importance because we previously decided to consider only the positive energies.

For $E=0$ in Fig. 13, the escape orbits and periodic bound orbits are available, which are illustrated in Figs. 14 and 15.

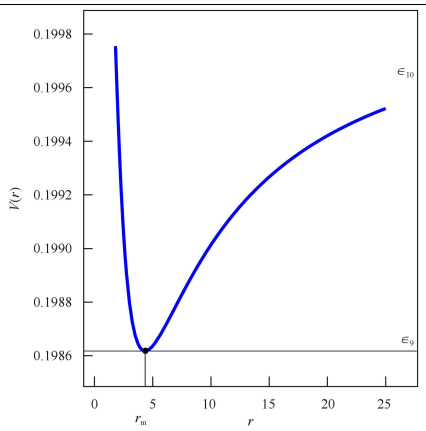

Fig. 17. The potential for a test-particle moving on a Type 2 Majumdar-Papapetrou star. The interior solution is Class Ia considering the first case $l=-kR^2$. The illustration is plotted for $Q_0=1$, $q=0.18$, $m=0.2$, $L=0.124$, $r_0=2$, $\delta r=0.1r_0$. The unit of length along the coordinate axis is M.

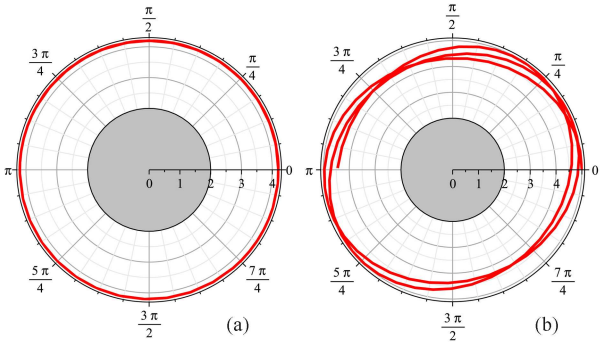

Fig. 18. The periodic bound orbits for a test-particle moving on a Type 2 Majumdar-Papapetrou star, using different initial points of approach when $E=0$: (a) $r=r_{\rm m}$, $E=\epsilon_9$; (b) $r=5$, $E=\epsilon_{10}$.

Also for higher energies, the periodic bound orbits are possible (Fig. 16).

II) The case $l=-kR^2$ (Type 2):

According to Eq. (59), the total charge is positive, therefore using Eqs. (55)–(57) we have:

$$q_0=m_0=\frac{(2r_0-|Q_0|)(r_0-\delta r)^3|Q_0|}{r_0^4}\left[\sqrt{\frac{r_0^4-2|Q_0|r_0^3+r_0^2Q_0^2+4|Q_0|r_0^2\delta r-2r_0\delta rQ_0^2-2|Q_0|\delta r^2r_0+\delta r^2Q_0^2}{r_0^4}}+1\right]^{-1}. \quad (61)$$

The potential in this case for the same data is plotted in Fig. 17 as in the previous case. This potential allows periodic bound orbits and escape orbit for the test-particle (Figs. 18 and 19).

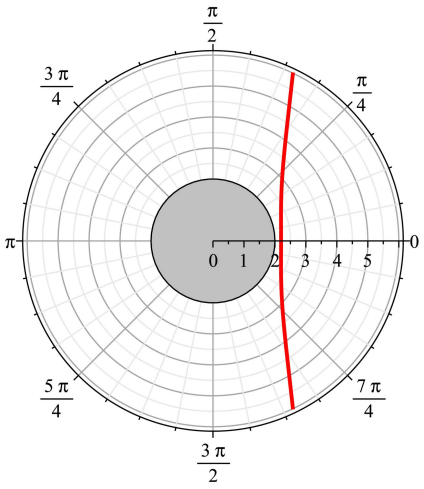

Fig. 19. The escape orbits for a test-particle moving on a Type 2 Majumdar-Papapetrou star for: $r=2.2$, $E=\epsilon_{10}$.

One can discover that for the default relation for $Q(r)$ in Eq. (55), the total charge of the star, has the possibility to be negative or positive. This depends somewhat on the mathematical relationship between the constant coefficients l and R^2. As we could see, this affects the test-particle trajectories and changes its possibilities to have various kinds of motions in each case.

7 Conclusion and discussion

Besides the differences between the shapes of orbits on different types of relativistic stars, there are other items, which can be used for more analytic comparisons. One of them is the period of stable orbits corresponding to the minimum energy $E_{\min}$, coinciding with the minimum of the potential curve at $r_{\rm m}$. From Eqs. (7) and (8), for example, the period of stable circular orbits in Class Ia, will be (see Appendix A):

$$T_{\rm Ia}=2\pi\frac{r_{\rm m}^2\left[C(r_{\rm m})+\sqrt{g(r_{\rm m})\left(m^2+\frac{\ell_{\rm Ia}^2}{r_{\rm m}^2}\right)}\right]}{g(r_{\rm m})\ell_{\rm Ia}^2}, \tag{62}$$

in which

$$\ell_{\rm Ia}=L|_{r=r_{\rm m}},$$

and $r_{\rm m}$ is indicated in Fig. 3. We can notice that:

$$r_{\rm m}|_{\rm Ib}<r_{\rm m}|_{\rm Ia},$$

and therefore

$$\ell_{\rm II}>\ell_{\rm Ib}>\ell_{\rm Ia}.$$

Note that, for the current data we have:

$$T_{\rm II}<T_{\rm Ib}<T_{\rm Ia}.$$

Another important item, useful to be compared between the cases, is the precession of periastron/apastron in periodic bound (planetary) orbits. For stable orbits, one can derive this precession as (see Appendix B):

$$\Delta\phi=\frac{2\pi}{\alpha}=2\pi\left[-6q_0^2u_{\rm m}^2+\frac{q^2q_0^2}{\ell_{\rm Ia}^2}+6m_0u_{\rm m}^2-1-\frac{m^2q_0^2}{\ell_{\rm Ia}^2}\right]^{\frac{1}{2}}, \tag{63}$$

which has been derived for known angular momentum, energy and the radius of stable orbits in Class Ia. We can conclude that:

$$\Delta\phi|_{\rm Ib}<\Delta\phi_{\rm Ia}.$$

In this article, we considered a relativistic charged perfect fluid as a relativistic spherical star, and reviewed the Guilfoyl's interior solutions, through comparing the motion of a massive charged particle on such a star. We investigated the effects of these interior solutions on the exterior geometry, for various types of relativistic stars, by studying the geodesic motions of a massive charged test-particle. We showed how changes in distributed charge and mass in a certain volume could affect the dynamical properties of the exterior geometry. We also plotted the potentials, and possible orbits, confirming that each case may exhibit peculiar shapes of orbits. We also discussed the special case of a pressure-less Majumdar-Papapetrou star, and illustrated the potentials and corresponding types of possible orbits.

I would like to thank Zahra Gh. Moghaddam, for her interest in this work.

Appendix A

Derivation of the period for stable orbits

In Eq. (13) we substitute:

$$E_{\min}=C(r_{\rm m})+\sqrt{g(r_{\rm m})\left(m^2+\frac{\ell_{\rm Ia}^2}{r_{\rm m}^2}\right)}. \tag{A1}$$

The Eqs. (7) and (8), for the current case can yield:

$$\frac{{\rm d}t}{{\rm d}\tau}=\frac{E_{\min}}{g(r_{\rm m})},$$

$$\frac{{\rm d}\phi}{{\rm d}\tau}=\frac{\ell_{\rm Ia}^2}{r_{\rm m}^2}.$$

To calculate its period we need the rate of changing in the coordinate time t with respect to ϕ as follows:

$$T=2\pi\frac{\mathrm{d}t}{\mathrm{d}\phi}. \tag{A2}$$

By chain differentiation we have:

$$\frac{\mathrm{d}t}{\mathrm{d}\phi}=\frac{\mathrm{d}t/\mathrm{d}\tau}{\mathrm{d}\phi/\mathrm{d}\tau}=\frac{E_{\min}/g(r_{\mathrm{m}})}{\ell_{\mathrm{Ia}}^2/r_{\mathrm{m}}^2}.$$

Therefore for the period of stable orbits in Class Ia, (from Eq. (A1)) we have:

$$T_{\mathrm{Ia}}=2\pi\frac{r_{\mathrm{m}}^2\left[C(r_{\mathrm{m}})+\sqrt{g(r_{\mathrm{m}})\left(m^2+\frac{\ell_{\mathrm{Ia}}^2}{r_{\mathrm{m}}^2}\right)}\right]}{g(r_{\mathrm{m}})\ell_{\mathrm{Ia}}^2}. \tag{A3}$$

Appendix B

Derivation of the precession of periastron in planetary orbits

We will find this precession here in the following way [26]: Substituting $u=\dfrac{1}{r}$ in Eq. (11) yields:

$$\left(\frac{\mathrm{d}u}{\mathrm{d}\phi}\right)^2 = -q_0^2u^4+2m_0u^3-u^2\left(1+\frac{q_0^2m^2}{L^2}\right) +\frac{2m_0m^2}{L^2}u+\frac{(E-qq_0u)^2-m^2}{L^2}. \tag{B1}$$

We consider an approximately stable orbit, with deviations on the trajectory. This helps us compare the trajectories with the known circular orbits and simplify the calculations to derive the precession. By defining:

$$z=u-u_{\mathrm{m}},$$

in which z is the deviation from circularity. We substitute this in Eq. (B1), ignoring the terms $O(z^3)$ because we are interested in nearly circular orbits ($z\ll1$). Considering $L=\ell_{\mathrm{Ia}}$ and $E=E_{\min}$ for the stable orbits in Class Ia, yields:

$$\begin{aligned}\left(\frac{\mathrm{d}z}{\mathrm{d}\phi}\right)^2 = &\left[-u_{\mathrm{m}}^2-u_{\mathrm{m}}^4q_0^2+\frac{E_{\min}^2}{\ell_{\mathrm{Ia}}^2}-\frac{m^2q_0^2u_{\mathrm{m}}^2}{\ell_{\mathrm{Ia}}^2}-\frac{2E_{\min}qq_0u_{\mathrm{m}}}{\ell_{\mathrm{Ia}}^2}\right.\\ &\left.+\frac{2m^2m_0^2u_{\mathrm{m}}}{\ell_{\mathrm{Ia}}^2}+2m_0u_{\mathrm{m}}^3+\frac{q^2q_0^2u_{\mathrm{m}}^2}{\ell_{\mathrm{Ia}}^2}-\frac{m^2}{\ell_{\mathrm{Ia}}^2}\right]\\ &+z\left[\frac{2q^2q_0^2u_{\mathrm{m}}}{\ell_{\mathrm{Ia}}^2}-4q_0^2u_{\mathrm{m}}^3-\frac{2m^2q_0^2u_{\mathrm{m}}}{\ell_{\mathrm{Ia}}^2}-2u_{\mathrm{m}}+6m_0u_{\mathrm{m}}^2\right.\\ &\left.-\frac{2E_{\min}qq_0}{\ell_{\mathrm{Ia}}^2}+\frac{2m^2m_0}{\ell_{\mathrm{Ia}}^2}\right]z^2\left[-6q_0^2u_{\mathrm{m}}^2+\frac{q^2q_0^2}{\ell_{\mathrm{Ia}}^2}\right.\\ &\left.+6m_0u_{\mathrm{m}}^2-1-\frac{m^2q_0^2}{\ell_{\mathrm{Ia}}^2}\right].\end{aligned} \tag{B2}$$

Here, we must have a periodic function, to return the initial ϕ and u after a period. As usual we choose $z=c_1+c_2\cos(\alpha\phi+c_3)$ in which c_1, c_2 and c_3 are constants. However, the coefficient α is not equal to one, and in Eq. (B2) it would be the square root of the coefficient of z^2 (see Ref. [26]). Therefore:

$$\alpha=\left[-6q_0^2u_{\mathrm{m}}^2+\frac{q^2q_0^2}{\ell_{\mathrm{Ia}}^2}+6m_0u_{\mathrm{m}}^2-1-\frac{m^2q_0^2}{\ell_{\mathrm{Ia}}^2}\right]^{\frac{1}{2}}. \tag{B3}$$

For $\alpha\phi=2\pi$, we have a complete orbit, therefore the change in ϕ from one periastron to the next is:

$$\Delta\phi=\frac{2\pi}{\alpha}=2\pi\left[-6q_0^2u_{\mathrm{m}}^2+\frac{q^2q_0^2}{\ell_{\mathrm{Ia}}^2}+6m_0u_{\mathrm{m}}^2-1-\frac{m^2q_0^2}{\ell_{\mathrm{Ia}}^2}\right]^{\frac{1}{2}}. \tag{B4}$$

References

1 Straumann N, Bieri L. Discovering the Expanding Universe. Cambridge: Cambridge University Press, 2009
2 Zel'dovich Ya B, Novikov I D. Relativistic Astrophysics, Vol. I: Stars and Relativity. Chicago: University of Chicago Press, 1971
3 Guilfoyle B S. Gen. Rel. Grav., 1999, **31**: 1645
4 ZHAI Xiang-Hau, YAUN Ning-Yi, LI Xin-Zhou. Chin. Phys. Lett., 1999, **16**(5): 321
5 Blaga P, Mioc V. Europhys. Lett., 1992, **17**(3): 275
6 Stuchlik Z. Bull. Astron. Inst. Czechosl., 1983, **34**: 129
7 Jorge C, Crispino Luís C B, Rodrigo R M et al. Braz. J. Phys., 2005, **35**(4B)
8 Prasanna A R, Vishveshwara C V. Pramana, 1978, **11**(4): 359
9 Chandrasekhar S. The Mathematical Theory of Black Holes. New York: Oxford University Press, 1983
10 Hackmann E, Lämmerzahl C. Phys. Rev. Lett., 2008, **100**: 171101
11 Hackmann E, Kagramanova V, Kunz J et al. Phys. Rev. D. 2008, **78**: 124018
12 Hackmann E, Kagramanova V, Kunz J et al. Europhys. Lett., 2009, **88**: 30008
13 Hackmann E, Lämmerzahl C, Kagramanova V et al. Phys. Rev. D, 2010, **81**: 044020
14 Hackmann E, Hartmann B, Lämmerzahl C et al. Phys. Rev. D, 2010, **81**: 064016
15 Kagramanova V, Kunz J, Hackmann E et al. Phys. Rev. D, 2010, **81**: 124044
16 Hackmann E, Hartmann B, Lämmerzahl C et al. Phys. Rev. D, 2010, **82**: 044024
17 Hackmann E, Lämmerzahl C. Phys. Rev. D, 2012, **85**: 044049
18 Wald Robert M. General Relativity. London: The University of Chicago Press, 1984
19 Nakahara M. Geometry, Topology and Physics. Second Edition. London: Ihstitute of Physics (IOP), 2003
20 Misner C W, Thorne K S, Wheeler J A. Gravitation. Freeman, 1973
21 Greiner W. Classical Mechanics: Sytem of Particles and Hamiltonian Dynamics. New York: Springer-Verlag, 2003
22 Weyl H. Ann. Phys. (Berlin), 1917, **359**: 117
23 Lemos Josè P S, Zanchin Vilson T. Phys. Rev. D, 2010, **81**: 124016
24 Majumdar S D. Phys. Rev., 1947, **72**: 390
25 Papapetrou A. Proc. R. Irish Acad. A, 1947, **51**: 191
26 Schutz Bernard F. A First Course in General Relativity. Second Edition. Cambridge: Cambridge University Press, 2009